

Supporting Information

Full parameter space exploration of microphase separation of block copolymer brushes within a single simulation framework

Tae-Yi Kim ^a, Ga Ryang Kang ^a, Myungwoong Kim ^{c,*}, Vikram Thapar ^{a,b,*}, Su-Mi Hur ^{a,b,*}

^a Department of Polymer Engineering, Graduate School, Chonnam National University,
Gwangju 61186, South Korea

^b Alan G. MacDiarmid Energy Research Institute & School of Polymer Science and
Engineering, Chonnam National University, Gwangju 61186, South Korea

^c Department of Chemistry and Chemical Engineering, Inha University, Incheon 22212,
South Korea

* Corresponding author E-mail: Su-Mi Hur: shur@chonnam.ac.kr, Vikram Thapar: thapar.09@gmail.com, Myungwoong Kim: mkim233@inha.ac.kr

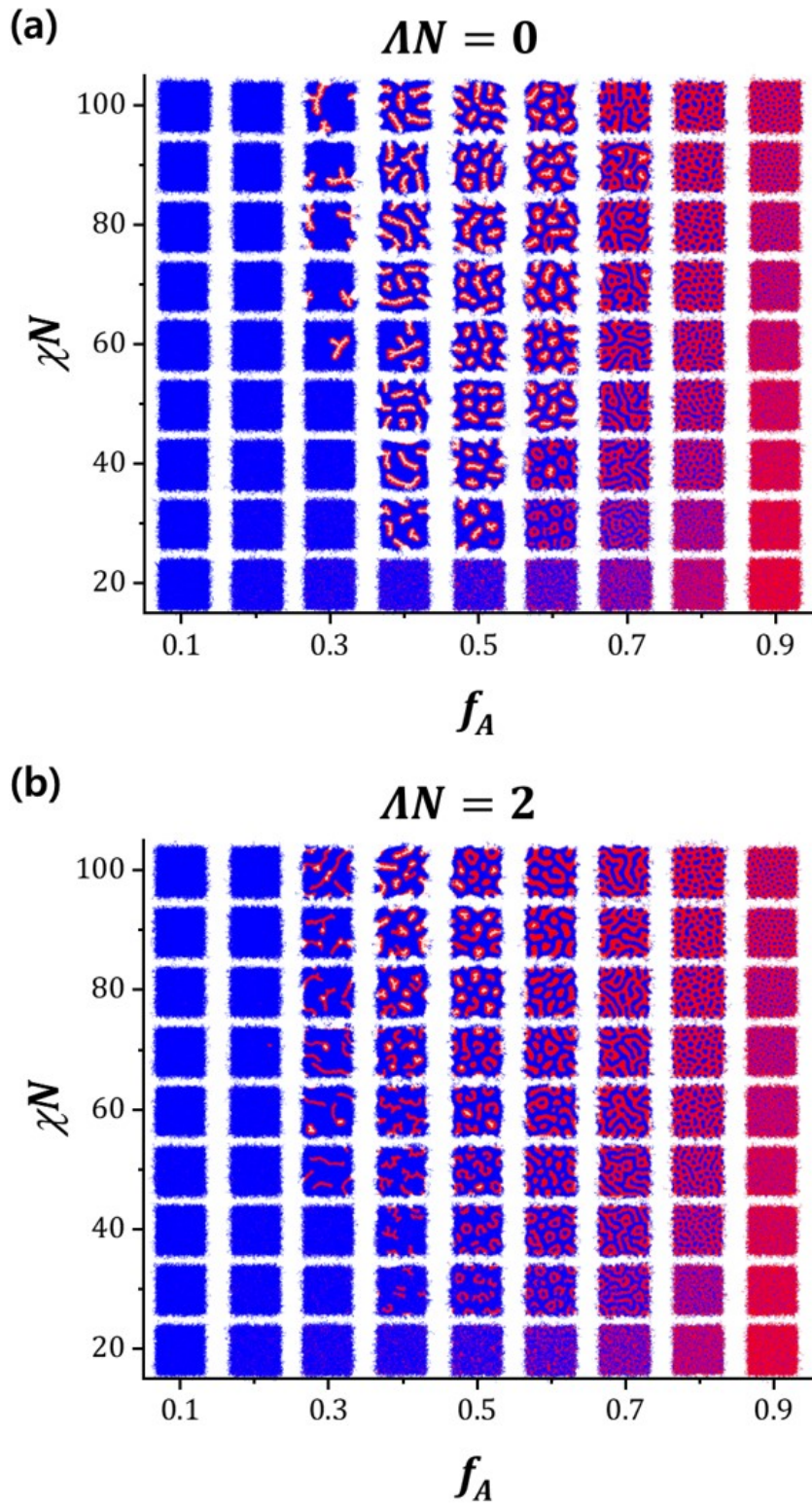


Figure S1: Top views of observed morphologies of AB diblock copolymer brushes as a function of the mole fraction of grafted block f_A and χN when it is grafted at the average brush thickness (L) = $0.5R_e$ on substrates of different wettability with (a) $\Delta N = 0$ and (b) $\Delta N = 2$. A and B blocks are represented by red and blue, respectively.

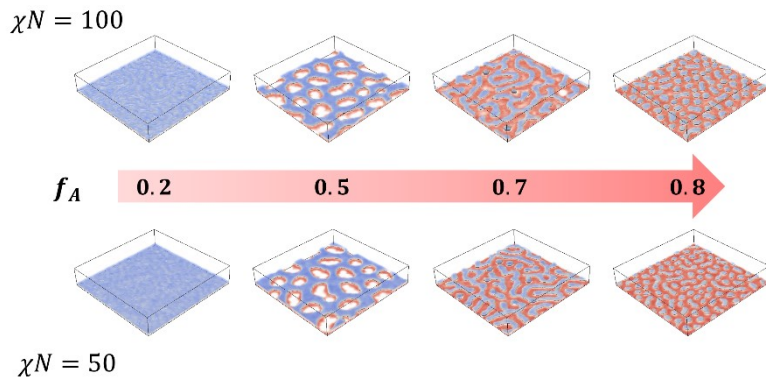


Figure S2: Representative morphologies in BCP brushes on the neutral substrate ($\Delta N = 0$) in the larger simulation box ($15R_e \times 15R_e$) at $\chi N = 50$ and 100 with varying f_A . A and B blocks are represented by red and slightly transparent blue, respectively, and the interface between A and B blocks is shown by gray.

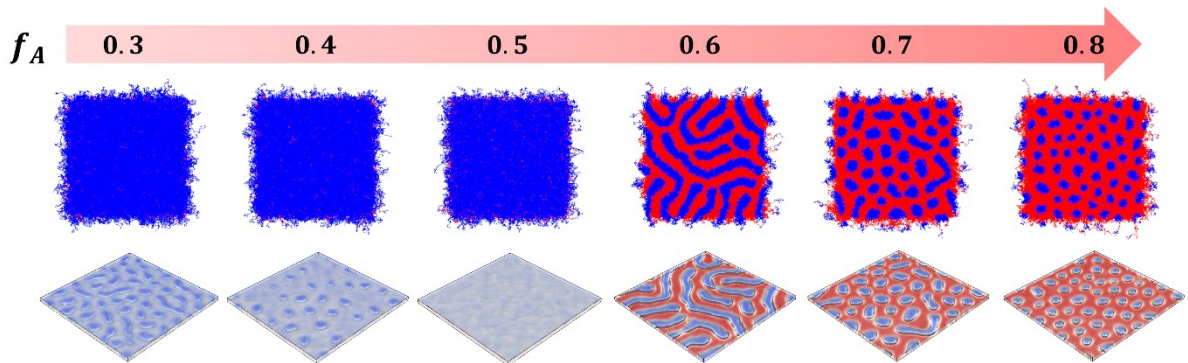


Figure S3: Top and tilted views of BCP brushes at different values of f_A , with a flat free surface constraint. Brush thickness L and χN are fixed at $0.5R_e$ and 50 , respectively. The interface between A and B in the tilted views is marked with gray color, while A and B blocks are marked in red and blue, respectively.

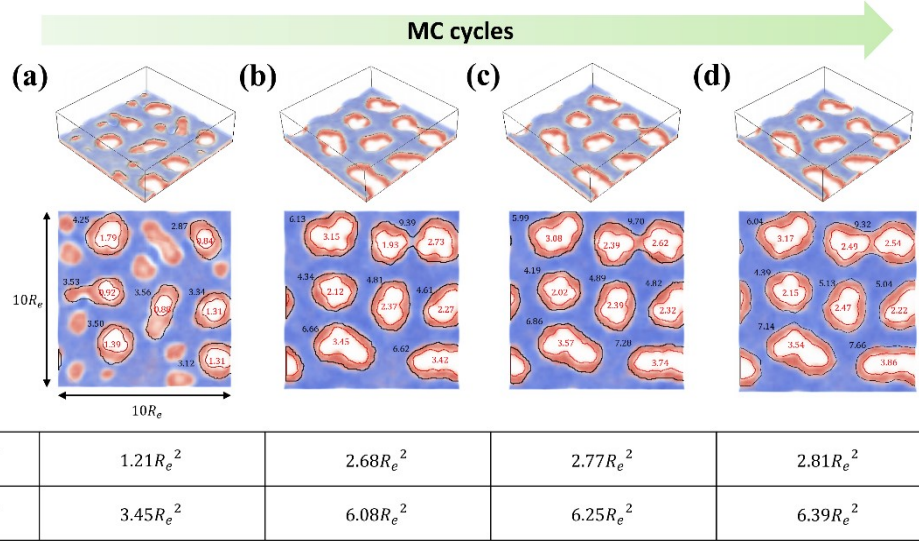


Figure S4: (a) - (d) Structure evolution of void phase at the later stage on a substrate of $\mathcal{AN} = 0$, along with measured numbers and area of voids. The dewetted (white) region is measured as the void size in the bottom, while the steep edge of the B(blue) domain is tracked to measure the void on the top. Variation on the average size of voids on the bottom substrate and from the top surface in each snapshot are summarized in the table. The average brush thickness (L), segregation strength (χN) and mole fraction (f_A) of systems are set to $0.5R_e$, 50 and 0.5, respectively.

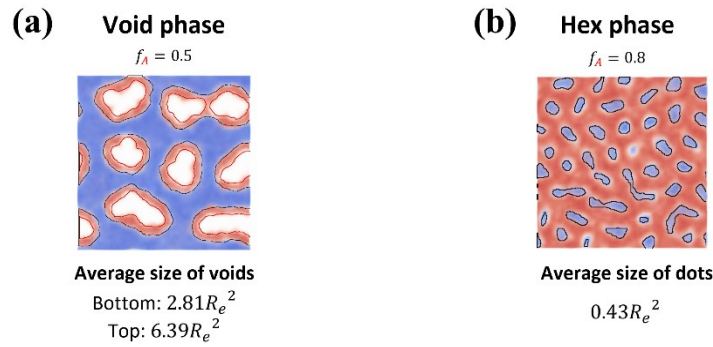


Figure S5: Comparison on the average size of (a) voids in an equilibrated void phase at $f_A = 0.5$ and (b) dots in a hex phase at $f_A = 0.8$ at the same other system variables, $L = 0.5R_e$, $\chi N = 50$, $\kappa N = 200$ and $\mathcal{AN} = 0$.

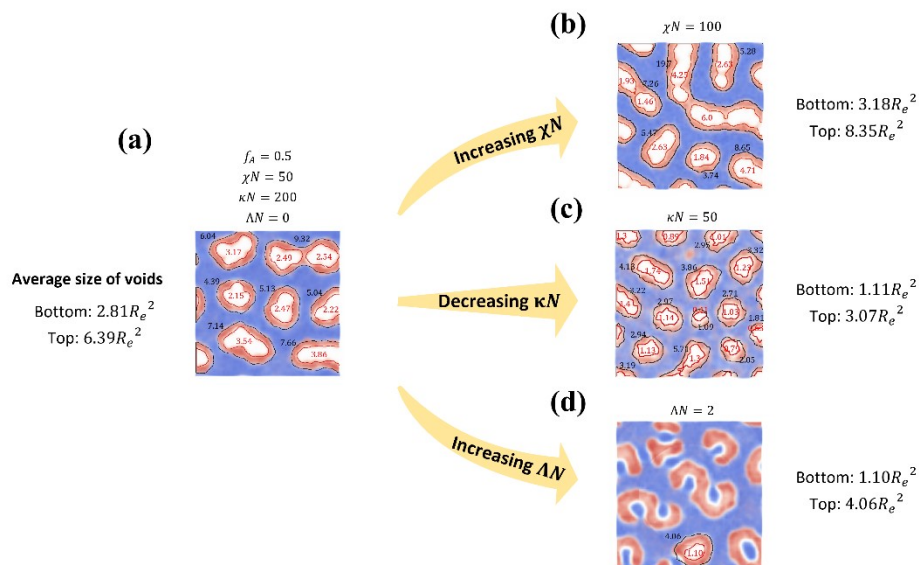


Figure S6: Variations on the average size of voids in (a) BCP brush of $L = 0.5R_e$ and $f_A = 0.5$ on a substrate of $\Delta N = 0$ when (b) increasing segregation strength(χN) from 50 to 100, (c) decreasing top surface affinity(κN) from 200 to 50, and increasing (d) substrate affinity(ΔN) from 0 to 2.

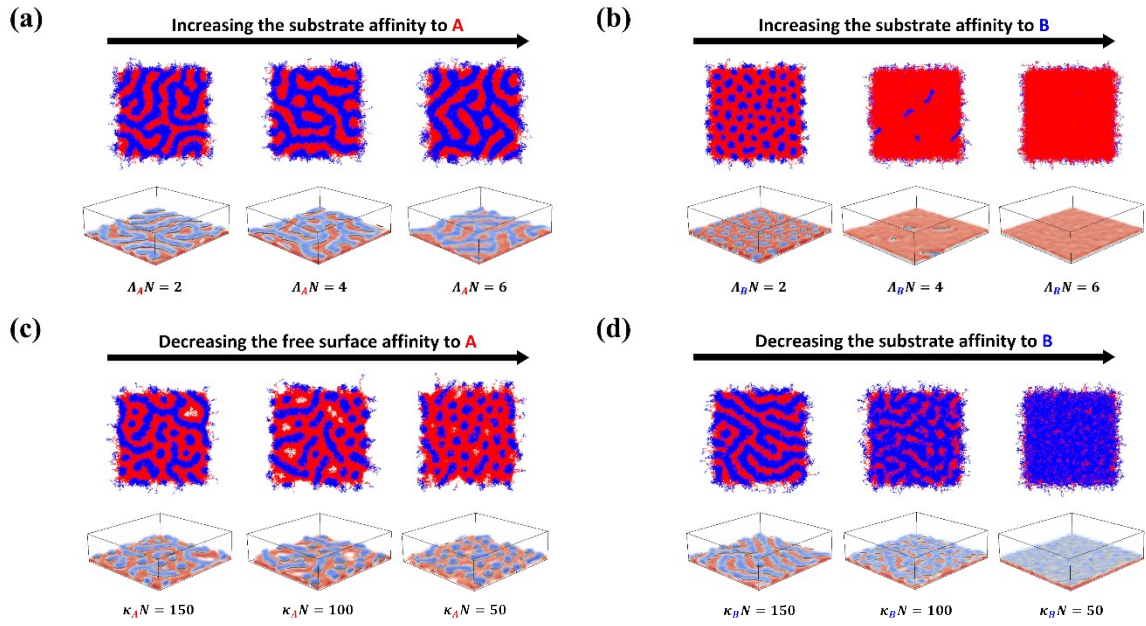


Figure S7: Top and tilted views of morphologies presenting the effects of selective affinity of surfaces on stripe phase. With BCP brushes at $f_A = 0.7$, $\Lambda_A N = \Lambda_B N = 0$ and $\kappa_A N = \kappa_B N = 200$ as a reference, simulations are conducted as increasing preferential wetting on the grafting substrate toward (a) A blocks (increasing $\Lambda_A N$ from 2 to 6 with fixed $\Lambda_B N = 0$) or (b) B blocks (increasing $\Lambda_B N$ from 2 to 6 with fixing $\Lambda_A N = 0$), or by increasing preferential wetting on the free surface toward (c) A blocks (decreasing $\kappa_A N$ from 150 to 50 with fixed $\kappa_B N = 200$) or (d) B blocks (decreasing $\kappa_B N$ from 150 to 50 at $\kappa_A N = 200$).

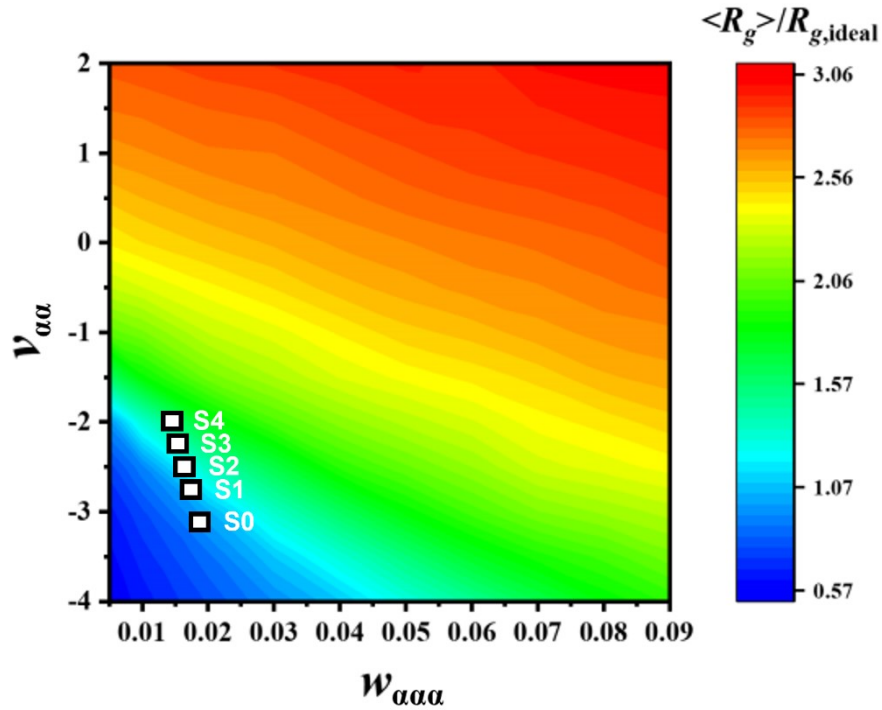


Figure S8: Colormap of the averaged radius of gyration relative to the size of an ideal chain, $\langle R_g \rangle / R_{g,ideal}$, on the model parameter space of $v_{\alpha\alpha}$ and $w_{\alpha\alpha\alpha}$. Squares represent model parameters used for different solvent qualities from S0 (melt) to S4. The figure is adapted from Figure S1 in ref 49.

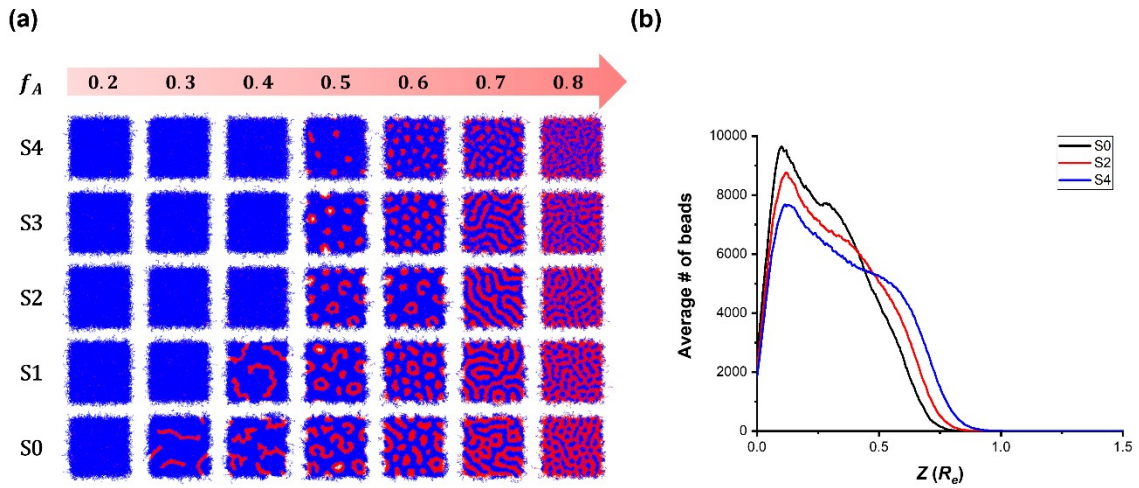


Figure S9: (a) Phase diagram presented with top views of BCP brushes with varying solvent quality from S0(melt) to S4 and composition f_A , at fixed $L = 0.5R_e$, $\Delta N = 2$ and $\chi N = 50$. (b) Variation of the average number of beads along the z direction in the brushes of $f_A = 0.7$, exposed to S0, S2 and S4. Black, red and blue lines represent density profiles under S0, S2 and S4, respectively.